2012

Analysis of π-Phase-Shifted Fiber Bragg Gratings for Ultrasonic Detection

Tongqing Liu
University of Nebraska-Lincoln, tongqing@huskers.unl.edu

Ming Han
University of Nebraska-Lincoln, mhan3@unl.edu

Analysis of π-Phase-Shifted Fiber Bragg Gratings for Ultrasonic Detection

Tongqing Liu and Ming Han, *Member, IEEE*

***Abstract*— Using numerical simulations, we investigated the responses of the π-phase-shifted fiber Bragg gratings (πFBGs) impinged by pressure ultrasonic waves. The effect of the grating length, grating refractive index modification depth, and ultrasonic frequency on the wavelength sensitivity and intensity sensitivity of the πFBG ultrasonic sensor for ultrasonic waves of different wavelengths was analyzed. The directivity of a πFBG sensor was also studied. Our analysis revealed several unique πFBG response characteristics and will be useful in the design and optimization of fiber-optic ultrasonic sensors that use a πFBG as the sensing element.**

***Index Terms*— Fiber Bragg grating (FBG), fiber-optic sensors, pressure wave, ultrasonic detection.**

I. Introduction

ULTRASONIC sensor applications are found in a variety of areas such as nondestructive structural health monitoring and medicine. Traditional ultrasonic sensors are typically based on piezoelectric ceramics. Fiber-optic ultrasonic sensors, particularly fiber Bragg grating (FBG)-based ultrasonic sensors, offer many advantages compared to their electronic counterparts. They are small, lightweight, and can be easily embedded into a structure without having any adverse impact on the mechanical properties of the structure. In addition, fiber-optic sensors are durable and immune to electromagnetic interference. Moreover, FBG-based sensors offer excellent multiplexing capabilities. Many FBGs can be fabricated on a single fiber to perform ultrasonic detection at multiple locations resulting in reduced cost and large coverage.

Ultrasonic detection based on regular FBGs has been extensively studied during the past few decades [1-5]. FBG ultrasonic detection typically relies on detecting a shift in the FBG's reflection spectrum caused by ultrasonic waves using a narrow linewidth laser whose wavelength is locked to the middle-reflection wavelength of the spectrum. The detection sensitivity is limited by the spectral slopes. A special type of FBGs whose reflection spectrum features a notch caused by a π-phase discontinuity in the center of the grating (called π-phase-shifted FBGs or πFBGs) have attracted a great deal of attention for their highly sensitive ultrasonic detection [6, 7]. Due to the phase discontinuity, a πFBG can be conceptually considered to be a Fabry–Perot cavity formed by two FBG mirrors. When the two FBGs are highly reflective, the quality factor of the Fabry–Perot cavity is increased, leading to an extremely narrow spectral notch for highly sensitive ultrasonic detection. Although ultrasonic detection based on πFBGs has been demonstrated, the response of πFBG sensors to ultrasonic waves has not been fully studied.

In this paper, we present the use of πFBGs as a sensing element for ultrasonic detection and investigate the behavior of πFBGs, including the Bragg wavelength shift, detection sensitivity, and directivity, when the sensor is impinged with ultrasonic pressure waves of different wavelengths. Our analysis will unveil several distinct differences between the responses of πFBGs and regular FBGs and is of importance to the understanding and design of πFBG-based ultrasonic sensors. The paper is organized as follows: first, a straightforward theory to simulate the reflection spectrum of a πFBG impinged by an ultrasound wave is presented in Section 2; then, the simulation results on the Bragg wavelength shift, sensor detection sensitivity, and directivity for πFBGs of different designs are given in Section 3; finally, several conclusions are provided in Section 4.

II. Modeling

The schematic of a πFBG is shown in Fig. 1(a). It consists of a phase jump of π at the center of an otherwise periodic modification of the refractive index in the core of a single-mode fiber. The phase jump leads to a spectral notch at the center of the reflection bandwidth of the grating. The spectral position of the dip, which is the Bragg wavelength (λ_B) of the grating, is given by

$$\lambda_B = 2n_{eff}\Lambda_0 \tag{1}$$

where n_{eff} is the effective refractive index of the optical mode propagating along the fiber, and Λ_0 is the grating period. When the πFBG is impinged by ultrasonic waves, the mechanical strain induced to the fiber will change the grating period as well as the refractive index of the fiber through the elasto-optic effect, causing a shift to the Bragg wavelength. Therefore, the ultrasonic waves can be detected by monitoring the ultrasonically induced πFBG spectral shift. This monitoring typically consists of measuring the reflection of a narrow-linewidth laser whose wavelength is set at the center of the linear range of the spectral dip, as shown in Fig. 1(b).

Manuscript received November 17, 2011; revised February 22, 2012; accepted February 23, 2012. Date of publication March 6, 2012; date of current version May 24, 2012. This work was supported in part by the U.S. Office of Naval Research under Grant N000141110262 and Grant N000141110499. The associate editor coordinating the review of this paper and approving it for publication was Prof. Julian C. C. Chan.

The authors are with the University of Nebraska-Lincoln, Lincoln, NE 68588-0511 USA (e-mail: mhan3@ unl.edu; tongqing@huskers.unl.edu).

Color versions of one or more of the figures in this paper are available online at http://ieeexplore.ieee.org.

Digital Object Identifier 10.1109/JSEN.2012.2189383

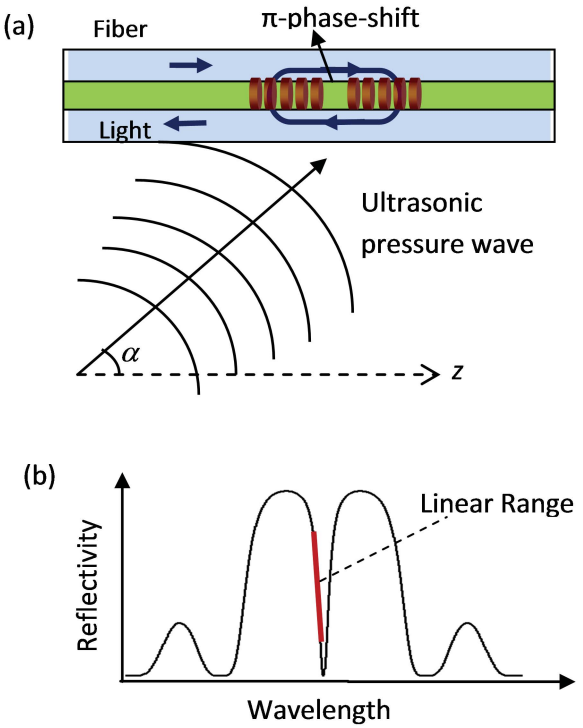

Fig. 1. (a) Schematic of a πFBG and an ultrasonic pressure wave impinging onto the grating with an incident angle of α. (b) Schematic of the reflection spectrum of a πFBG.

For simplicity, we assume that the πFBG is impinged by a plane pressure wave with a propagation direction parallel to the fiber [$\alpha = 0°$ in Fig. 1(b)], whose differential pressure field, ΔP, is given by

$$\Delta P(z,t) = \Delta P_0 \cos\left(\omega t - \frac{2\pi}{\lambda_S} z\right) \tag{2}$$

where ΔP_0, ω, and λ_s are, respectively, the peak pressure, the angular frequency, and the wavelength of the ultrasonic wave; z is the coordinate along the fiber direction; and t is the time. Pressure waves with different impinging angles will be discussed in Section 3. We further assume that the acoustic impedance of the πFBG is perfectly matched to the medium in which the πFBG is embedded, so that the ultrasonic reflections and diffractions at the boundary between the fiber and the medium and the guided ultrasonic waves in the fiber are not considered here. As a result, (2) is also valid for describing the pressure field inside the πFBG.

The relative changes to the refractive index and the grating period due to the pressure wave in the fiber can be written as [4, 8]

$$\frac{\Delta n(z,t)}{n_{eff}} = n^2 \frac{\Delta P(z,t)}{2E}(1-2\upsilon)(2P_{12}+P_{11}) \tag{3}$$

$$\frac{\Delta \Lambda(z,t)}{\Lambda_0} = -\frac{\Delta P(z,t)(1-2\upsilon)}{E} \tag{4}$$

where E and υ are the Young's modulus and the Poisson's ratio; and P_{11} and P_{12} are the two independent elements of the strain-optic tensor for the πFBG material [9]. Assuming that the πFBG is uniform with a refractive index modulation depth of δn_0, the index change and the grating period modified by the ultrasonic waves are given by

$$\delta n(z,t) = \delta n_0 + \Delta n(z,t) \tag{5}$$

$$\Lambda(z,t) = \Lambda_0 + \Delta\Lambda(z,t). \tag{6}$$

Apparently, for low frequency ultrasonic waves whose wavelengths are much larger than the length of the πFBG, the perturbations are approximately uniform and can be regarded as a constant tensile strain or compressive strain over the πFBG length at a given time. As the wavelength of the ultrasonic wave is comparable to or shorter than the πFBG length, the perturbations become nonuniform; and numerical methods have to be used to find the spectral shift of the dip.

We use a piecewise-uniform approach derived from coupled-mode theory to model the reflection spectrum of a πFBG impinged by ultrasonic waves. In such a model [10, 11], the grating is divided into M sessions, each of which can be considered as a uniform grating with the refractive index change and grating period described by (5) and (6) at the position of the session. The complex amplitudes of the optical modes before and after the i^{th} uniform grating session are related by a 2×2 matrix F_i such as [10]

$$\begin{bmatrix} R_i \\ S_i \end{bmatrix} = F_i \begin{bmatrix} R_{i-1} \\ S_{i-1} \end{bmatrix} = \begin{bmatrix} F_{11} & F_{12} \\ F_{21} & F_{22} \end{bmatrix} \begin{bmatrix} R_{i-1} \\ S_{i-1} \end{bmatrix} \tag{7}$$

where R_i and S_i are the complex amplitudes of the forward and backward traveling modes after the i^{th} session, and the elements in F_i are defined by [10]

$$F_{11} = F_{22}^* = \cosh(\gamma_B \Delta z) - i\frac{\hat{\sigma}}{\gamma_B}\sinh(\gamma_B \Delta z) \tag{8}$$

$$F_{12} = F_{21}^* = -i\frac{\kappa}{\gamma_B}\sinh(\gamma_B \Delta z) \tag{9}$$

where "*" denotes complex conjugate. In (8) and (9), Δz is the length of the i^{th} uniform section, κ is the coupling coefficient, $\hat{\sigma}$ is a general "dc" self-coupling coefficient, and $\gamma_B = (\kappa^2 - \hat{\sigma}^2)^{1/2}$. For single-mode reflection gratings, like the πFBG discussed here, $\kappa = \pi\delta n(z)/\lambda$ and $\hat{\sigma} = 2\pi n_{eff}(1/\lambda - 1/\lambda_D) + 2\pi\delta n(z)/\lambda$, where λ is the optical wavelength and $\lambda_D = 2n_{eff}\Lambda(z)$. Multiplying all of the matrices for individual sessions will give a single 2×2 matrix for the whole grating so that

$$\begin{bmatrix} R_M \\ S_M \end{bmatrix} = F \begin{bmatrix} R_0 \\ S_0 \end{bmatrix} \tag{10}$$

where $F = F_M \cdot F_{M-1} \cdots F_1$. To account for the π-phase shift, a phase-shift matrix, F_{pi}, given by

$$F_{pi} = \begin{bmatrix} -i & 0 \\ 0 & i \end{bmatrix} \tag{11}$$

can be inserted at the position of the phase shift. With boundary conditions at the end of the πFBG, such as $R_0 = R(L) = 1$ and $S_0 = S(L) = 0$, where L is the length of the grating, the complex amplitudes at the start of the πFBG, R_M and S_M, can be obtained. Consequently, the amplitude reflection coefficient and power reflectivity of the πFBG can be calculated by $r = R_M/S_M$ and $R_p = |r|^2$, respectively.

III. Results and Discussion

The model described above simulates the reflection spectrum of πFBGs impinged by a pressure wave, given by (2), which allows us to study the performance of πFBGs when they are used as ultrasonic sensors. The key parameters of sensor performance, including sensitivity and frequency response, and the directivity of the πFBG ultrasonic sensors with different grating parameters, are discussed in this section. In our analysis, the unperturbed Bragg wavelength of the πFBGs is 1550 nm with $n_{eff} = 1.4453$; and the πFBG material is assumed to be fused silica with relevant parameters of $E = 70$ GPa, $\nu = 0.17$, $p_{11} = 0.121$, and $p_{12} = 0.270$.

A. Sensitivity and Frequency Response

Here we define two types of sensor sensitivity to ultrasonic waves. The first is called "wavelength sensitivity," which is defined by the maximum spectral shift of the πFBG Bragg wavelength caused by an ultrasonic wave with unity pressure amplitude. The second is called "intensity sensitivity," which is defined by the reflectivity change at the center position of the linear range (50% reflection) of the πFBG reflection spectrum caused by an ultrasonic wave with unity pressure amplitude. The intensity sensitivity is more relevant from a practical standpoint because it represents the sensitivity of a laser-based πFBG ultrasonic sensor system that uses a laser with its wavelength locked to the 50% reflection position. The intensity sensitivity is determined not only by the wavelength sensitivity but also by the slope of the πFBG spectral linear range. Therefore, the wavelength sensitivity and intensity sensitivity are analyzed separately.

Fig. 2(a) shows the wavelength sensitivity as a function of the ultrasonic wavenumber for πFBGs with lengths (L) ranging from 2–10 mm. We assume that the πFBGs have the same refractive index modulation depth $\delta n_0 = 1 \times 10^{-4}$. Note that the frequency of an ultrasonic wave is proportional to its wavelength for a given material. The wavelength sensitivity of all of the πFBGs starts from the same maximum of 4.5 pm/MPa when the ultrasonic wavenumber is zero and decreases as the ultrasonic wavenumber increases, with the sidelopes appearing at the tail of the curves. At low wavenumber ranges, the wavelength sensitivity of longer πFBGs drops more quickly to their first local minimum. This is because when the ultrasonic wavenumber increases, the ultrasonic wavelength becomes shorter; and the average changes to the refractive index and the grating period within the grating length caused by the ultrasonic waves decreases. This "averaging effect" is more evident in Fig. 2(b), which plots wavelength sensitivity as a function of the normalized ultrasonic wavenumber defined as the grating length-ultrasonic wavelength ratio (L/λ_S). All of the πFBGs fall to their first minimum at approximately the same value of L/λ_S. It is worth noting, from Fig. 2(a) and (b), that the first minimum occurs when the ultrasonic wavelength is twice the grating length ($L/\lambda_S = 2$); while the first minimum for a regular FBG occurs when $L/\lambda_S = 1.3$[5]. Therefore, a πFBG has a larger ultrasonic bandwidth compared to a regular FBG of the same length. The difference arises from the different

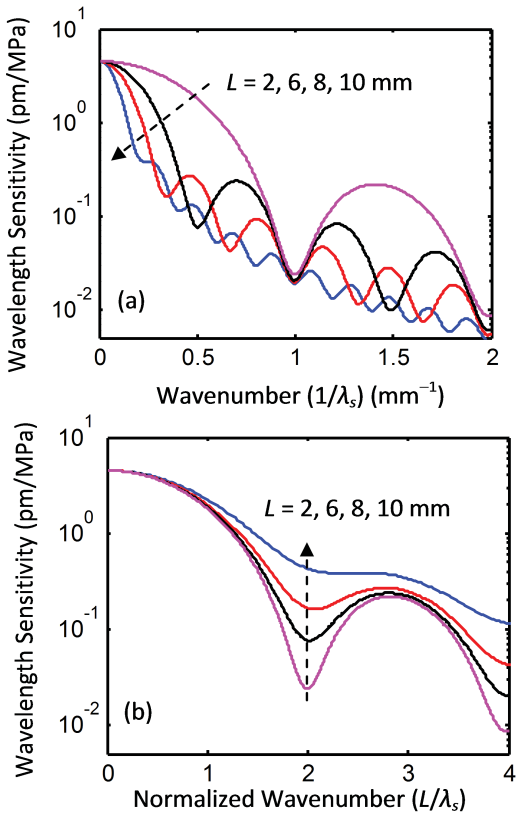

Fig. 2. Wavelength sensitivity response of πFBG with $\delta n_0 = 1 \times 10^{-4}$ and different lengths. (a) Wavelength sensitivity versus ultrasonic wavenumber. (b) Wavelength sensitivity versus normalized ultrasonic wavenumber.

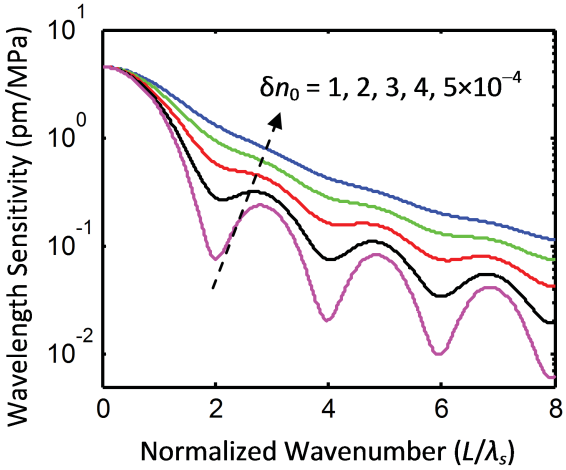

Fig. 3. Wavelength sensitivity response of 4-mm long πFBGs of different refractive index modification depths as a function of normalized ultrasonic wavenumbers.

spatial distributions of the light intensity along a πFBG and a regular FBG, which will be discussed further later in this section.

We also studied the effect of the refractive index modulation depth on the wavelength sensitivity of πFBGs, as shown in Fig. 3, which plots wavelength sensitivity as a function of the normalized ultrasonic wavenumber for πFBGs of the same length (4 mm) but with different refractive index modification

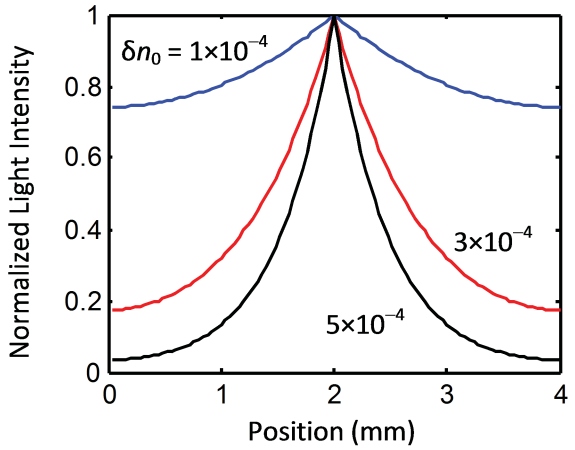

Fig. 4. Spatial distribution of the normalized light intensity over 4-mm long πFBGs of different refractive index modification depths.

depths (δn_0). Our results reveal that at higher ultrasonic frequencies, the wavelength sensitivity can be significantly enhanced by larger refractive index modification depths of the πFBGs. For example, at a frequency of 2 MHz, when the $\delta n_0 = 1 \times 10^{-4}$, the wavelength sensitivity is 0.076 pm/MPa. The wavelength sensitivity is increased to 0.59 pm/MPa for a $\delta n_0 = 3\times10^{-4}$. The wavelength sensitivity is further increased to 1.33 pm/MPa for a $\delta n_0 = 5 \times 10^{-4}$, which is almost 20 times better than for $\delta n_0 = 1 \times 10^{-4}$. The significantly enhanced wavelength sensitivity to ultrasonic waves observed in πFBGs is not present in regular FBGs. We also noticed that the sidelope structures of the wavelength sensitivity vs. normalized wavenumber curve are only evident for smaller refractive index modification depths, and the sidelopes become less visible for larger refractive index modification depths.

The reason for the sensitivity enhancement is that as a πFBG can be considered to be a Fabry–Perot cavity formed by two regular FBG mirrors, a larger refractive index modification depth yields a higher reflectivity of each of the FBG mirrors, leading to a higher cavity quality factor and a better spatial confinement of the light around the center of the πFBG, thereby reducing the "effective length" of the πFBG. As clearly seen in Fig. 4, which shows the light intensity distribution in the πFBGs of different refractive index changes, more light energy is distributed around the center of a πFBG with a larger refractive index modification depth. The unique light energy distribution in πFBGs is also responsible for the larger ultrasonic bandwidth of a πFBG compared to a regular FBG, as mentioned earlier this section.

In addition to wavelength sensitivity, we studied the intensity sensitivity of a laser-based πFBG ultrasonic sensor system. In particular, we considered the effect of the πFBG length on the intensity sensitivity and the ultrasonic frequency response of πFBGs. The intensity sensitivity is proportional to both the wavelength sensitivity and the slope of the linear range in the πFBG reflection spectrum. As discussed earlier, a longer πFBG length reduces the wavelength sensitivity due to the nonuniform perturbations to the refractive index and the grating pitch over the grating length. However, a longer

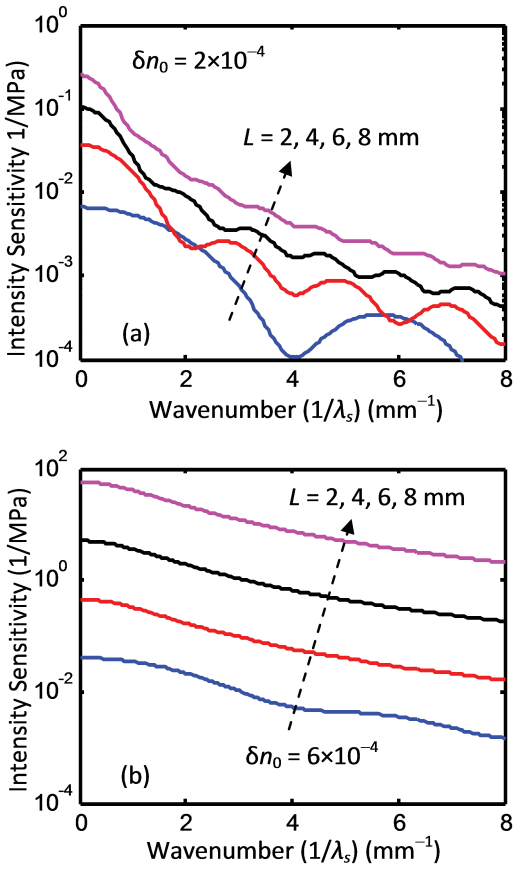

Fig. 5. Intensity sensitivity as a function of ultrasonic wavenumber for πFBGs of different refractive index modification depths (a) $\delta n_0 = 2 \times 10^{-4}$ and (b) $\delta n_0 = 6 \times 10^{-4}$.

πFBG length also reduces the bandwidth of the reflection spectral dip and increases the slope of the linear range. It is, therefore, worth studying the overall effect of the πFBG length on the intensity sensitivity. Fig. 5 (a) shows the intensity sensitivity as a function of the ultrasonic wavenumber for πFBGs of different lengths with the same refractive index modification depth of $\delta n_0 = 2 \times 10^{-4}$, which indicates that the intensity sensitivity of a longer πFBG is usually higher than that of a shorter πFBG. The benefit to the intensity sensitivity of longer πFBG lengths is more prominent in πFBGs with higher refractive index modification depths, as shown in Fig. 5 (b), which plots the intensity sensitivity vs. wavenumber for πFBGs with $\delta n_0 = 6 \times 10^{-4}$. We conclude, therefore, that increasing the πFBG length can increase the detection sensitivity of a πFBG ultrasonic sensor system as the increased spectral slope overcomes the reduced spectral sensitivity with a longer grating length. In practice, however, the πFBG length design also requires other considerations, e.g., the measurement range, the size of the ultrasonic beam to be detected, and the frequency noise of the laser. In addition, as shown below, a longer πFBG length makes the ultrasonic sensor highly directional, which is typically undesirable.

B. Directivity

Directivity is another important parameter for an ultrasonic sensor. So far, we have assumed that the direction of the

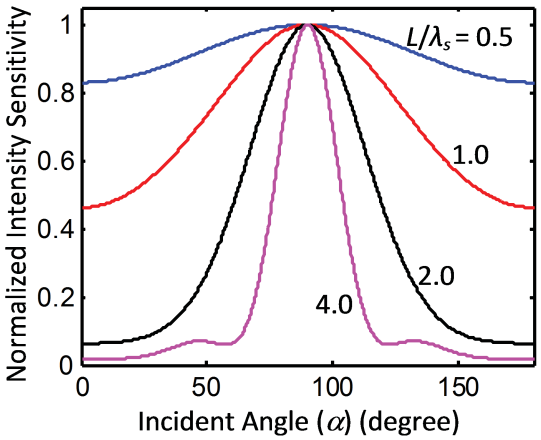

Fig. 6. Normalized intensity sensitivity as a function of ultrasonic incident angle for 4-mm long πFBG with a refractive index modification depth $\delta n_0 = 2 \times 10^{-4}$ impinged by ultrasonic waves of different wavelength.

ultrasonic pressure wave impinged onto the πFBG is parallel with the fiber axis. For the pressure wave given by (2) that impinges onto the πFBG at an angle of α with respect to the fiber axis, as shown in Fig. 1(a), the ultrasonic wavelength along the fiber axis direction is increased to

$$\lambda_\alpha = \frac{\lambda_S}{|\cos\alpha|} \tag{12}$$

while the amplitudes of the refractive index and the grating pitch modifications induced by the ultrasonic pressure wave remain unchanged. Therefore, the directivity of a πFBG ultrasonic sensor is expected to be highly dependent on the ratio between the grating length and the ultrasonic wavelength. When the ultrasonic wavelength is significantly larger than the grating length, the ultrasonic perturbation to the grating can be considered to be uniform; and the πFBG sensor should have an omnidirectional response. On the other hand, when the ultrasonic wavelength is smaller than the grating length, the πFBG sensor is highly directional with the maximum occurring at the normal incidence ($\alpha = 90°$) when the ultrasonic perturbation is uniform over the grating length. Fig. 6 shows the intensity sensitivity of a 4-mm πFBG with $\delta n_0 = 2\times10^{-4}$ as a function of incidence angle for different grating lengths to ultrasonic wavelength ratios, which clearly shows the strong directivity of a πFBG at high ultrasonic frequencies. For instance, when $L/\lambda_S = 4$, the sensitivity is about 50 times more sensitive for normal incidence than for parallel incidence. Recalling that increasing the fiber length can enhance the intensity sensitivity, the tradeoff between sensitivity and directivity must be considered in designing the πFBG length.

Similar directivity characteristics are also observed in other types of fiber-optic sensors, such as those based on Fabry–Perot cavities [12] and Sagnac interferometers [13]. It is worth noting that the above directivity analysis is only valid for an ultrasonic wave with an isotropic stress field, such as the pressure wave discussed in this paper. For ultrasonic waves in solids with an anisotropic stress field, the directivity analysis is much more complicated due to the fact that in addition to the dependence of the wavelength along the fiber axis on the incidence angle, the amplitudes of refractive index and grating pitch modifications induced by the ultrasonic wave are also dependent on the incidence angle. As a result, a grating ultrasonic sensor may show completely different directivity patterns. For example, it has been reported that in detection of Lamb waves in a solid plate, the sensitivity of a regular FBG sensor is a cosine function of the incidence angle with minimum sensitivity that occurs at normal incidence of the Lamb wave [14].

IV. Conclusion

A theoretical model has been established to simulate the responses of πFBGs impinged by ultrasonic pressure waves. In this model, the pressure field of the ultrasonic wave is described by a sinusoidal function and induces modifications to the grating pitch and fiber refractive index proportional to the pressure along the fiber axis. The πFBG is modeled by the transfer matrix method, in which the grating is divided into a number of uniform subsections, each associated with a 2×2 matrix; and a phase shift matrix accounts for the π phase shift of the grating. Although our analysis is performed on πFBGs impinged by a pressure ultrasonic field, the model is general and sufficient to describe the effect of any type of ultrasonic wave on fiber gratings.

Our analysis shows that, for a given πFBG, both the wavelength sensitivity and intensity sensitivity decrease as the ultrasonic frequency increases. For a given ultrasonic wave, the wavelength sensitivity decreases as the πFBG length increases. However, the intensity sensitivity can be enhanced by increasing the πFBG length as the increased slope of the πFBG spectral linear range overcomes the reduced wavelength sensitivity from a longer grating length. Our analysis reveals that the wavelength sensitivity of a πFBG can be increased by a larger refractive index modification depth of the grating, which provides tighter confinement to the light field and reduces the effective length of the grating. We also analyzed the directivity of a πFBG ultrasonic sensor for pressure waves. When the πFBG length is much smaller than the ultrasonic wavelength, the πFBG is omnidirectional. As the πFBG length increases, the πFBG ultrasonic sensor becomes more directional with the maximum sensitivity occurring at the normal incidence of the ultrasonic wave. In conclusion, our model and analysis have revealed several significant differences between ultrasonic sensors based on πFBGs and regular FBGs and are of great importance for designing and optimizing fiber-optic ultrasonic sensors based on fiber gratings.

References

[1] N. E. Fisher, J. Surowiec, D. J. Webb, D. A. Jackson, L. Gavrilov, J. W. Hand, L. Zhang, and I. Bennion, "In-fibre Bragg gratings for ultrasonic medical applications," *Meas. Sci. Technol.*, vol. 8, no. 10, pp. 1050–1054, Oct. 1997.

[2] N. Takahashi, A. Hirose, and S. Takahashi, "Underwater acoustic sensor with fiber Bragg grating," *Opt. Rev.*, vol. 4, no. 6, pp. 691–694, Nov.–Dec. 1997.

[3] I. M. Perez, H. L. Cui, and E. Udd, "Acoustic emission detection using fiber Bragg gratings," *Proc. SPIE*, vol. 4328, pp. 209–215, Jan. 2001.

[4] P. Fomitchov and S. Krishnaswamy, "Response of a fiber Bragg grating ultrasonic sensor," *Opt. Eng.*, vol. 42, no. 4, pp. 956–963, Apr. 2003.
[5] A. Minardo, A. Cusano, R. Bernini, L. Zeni, and M. Giordano, "Response of fiber Bragg gratings to longitudinal ultrasonic waves," *IEEE Trans. Ultrason. Ferroelectr. Freq. Control*, vol. 52, no. 2, pp. 304–312, Feb. 2005.
[6] D. Gatti, G. Galzerano, D. Janner, S. Longhi, and P. Laporta, "Fiber strain sensor based on a π-phase-shifted Bragg grating and the Pound-Drever-Hall technique," *Opt. Exp.*, vol. 16, no. 3, pp. 1945–1950, Feb. 2008.
[7] A. Rosenthal, D. Razansky, and V. Ntziachristos, "High-sensitivity compact ultrasonic detector based on a pi-phase-shifted fiber Bragg grating," *Opt. Lett.*, vol. 36, no. 10, pp. 1833–1835, May 2011.
[8] G. B. Hocker, "Fiber-optic sensing of pressure and temperature," *Appl. Opt.*, vol. 18, no. 9, pp. 1445–1448, 1979.
[9] J. F. Nye, *Physical Properties of Crystals: Their Representation by Tensors and Matrices*. Oxford, U.K.: Clarendon Press, 1979.
[10] T. Erdogan, "Fiber grating spectra," *J. Lightw. Technol.*, vol. 15, no. 8, pp. 1277–1294, Aug. 1997.
[11] M. Yamada and K. Sakuda, "Analysis of almost-periodic distributed feedback slab wave-guides via a fundamental matrix approach," *Appl. Opt.*, vol. 26, no. 16, pp. 3474–3478, Aug. 1987.
[12] J. Dorighi, S. Krishnaswamy, and J. D. Achenbach, "Response of an embedded fiber optic ultrasound sensor," *J. Acoust. Soc. Amer.*, vol. 101, no. 1, pp. 257–263, Jan. 1997.
[13] P. A. Fomitchov, S. Krishnaswamy, and J. D. Achenbach, "Extrinsic and intrinsic fiber optic Sagnac ultrasound sensors," *Opt. Eng.*, vol. 39, no. 7, pp. 1972–1984, Jul. 2000.
[14] D. C. Betz, G. Thursby, B. Culshaw, and W. J. Staszwski, "Structural damage location with fiber Bragg grating rosettes and lamb waves," *Struct. Health Monitor. Int. J.*, vol. 6, no. 4, pp. 299–308, Dec. 2007.

Tongqing Liu received the B.S. degree from the Dalian University of Technology, Dalian, China, in 2009. He is currently pursuing the Ph.D. degree with the University of Nebraska-Lincoln, Lincoln.

His current research interests include optical fiber sensors for ultrasonic detection and fiber-optic chemical sensors.

Ming Han (M'11) received the Ph.D. degree in electrical engineering from Virginia Polytechnic Institute and State University, Blacksburg, in 2006.

He is currently an Assistant Professor with the Department of Electrical Engineering, University of Nebraska-Lincoln, Lincoln. His current research interests include optical, biological and chemical sensing, optical measurement under harsh environments, fully or quasi-distributed fiber-optic sensors, and micro/nano-photonic devices and structures.